

Degradation of AISI 314 Steel at Elevated Temperatures

Rodrigo Silva Lopes¹, Jorge Luis Braz Medeiros², Luciano Volcanoglo Biehl³,
José de Souza⁴, Elton Gimenez Rossini⁵, Carlos Otávio Damas Martins⁶

¹ Escola de Engenharia – Pós-graduação em Engenharia Mecânica – PPMec – FURG/RS.

² Escola de Engenharia – Pós-graduação em Engenharia Mecânica – PPMec – FURG/RS. Grupo de Estudos em Fabricação e Materiais da FURG/RS. Prof. Doutor em Ciências dos Materiais.

³ Escola de Engenharia – Pós-graduação em Engenharia Mecânica – PPMec – FURG/RS. Grupo de Estudos em Fabricação e Materiais da FURG/RS. Prof. Doutor em Ciências dos Materiais.

⁴ Fundação Escola Técnica Liberato Salzano Vieira da Cunha – DPPI. Prof. Doutor em Ciências dos Materiais.

⁵ Universidade Estadual do Rio Grande do Sul, Prof. Doutor em Engenharia Mecânica.

⁶ Universidade Federal do Sergipe, Prof. Doutor e Ciências dos Materiais.

Corresponding author. E-mail: jorge.braz@furg.br

Abstract

This work studies the behavior of AISI 314 steel subjected to an atmosphere rich in hydrocarbons at high temperatures, verifying the reasons that led to the collapse of stainless steel. The alloy was analyzed by optical emission spectrometry to determine the original composition and after its use in service. The research conditions took place at a temperature of 1200 °C. The Vickers microhardness test demonstrated a decrease in microhardness from the surface towards the core. With the use of Optical Microscopy (OM), Scanning Electron Microscopy (SEM) and Energy Dispersive Spectroscopy (EDS), it was possible to observe the presence of Cr segregations, along the grain boundaries, especially with the presence of Cr carbides. In the immersion corrosion test, the effect of precipitates on corrosion resistance was evaluated. The results obtained evidenced the presence of sensitization, silicon segregation and chemical unbalance of the steel. The formation of precipitates on the grain boundaries, reducing the corrosion resistance of the samples studied, in addition to decreasing the toughness of the material, causing catastrophic failure in service.

Keywords: AISI 314 steel, Hydrocarbon atmosphere, Metal degradation.

Date of Submission: 01-01-2022

Date of Acceptance: 10-01-2022

I. INTRODUCTION

Austenitic stainless steels have excellent mechanical properties, such as corrosion resistance, high heat resistance, low creep at high temperatures, and good toughness at low temperatures [1-2]. They have significant applications in several fields, from domestic utensils to industrial use, such as chemical and nuclear industries, in pressure vessels, reactors, among others [3].

The chemical industry had, therefore, at its disposal - since the advent of austenitic stainless steels, a range of applications at high temperatures for these steels, as well as its use in installations in aggressive media [4]. The discovery of austenitic stainless steels meant a breakthrough in the development of materials resistant to corrosion and oxidation. However, these steels are particularly susceptible to intergranular corrosion [5].

AISI 314 stainless steels are characterized by having a high silicon content in their composition, increasing their resistance to oxidation at elevated temperatures, thus being an appropriate material for services in heat treatment furnaces [6-7].

Austenitic stainless steels form the largest group of stainless steels in use, representing about 65 to 70% of the total produced [8-9]. Its basic composition level is 16 to 26% chromium, 6 to 22% nickel, 2 to 5% manganese and a maximum of 0.25% carbon [10-11]. Unlike ferritic, austenitic steels have several characteristics that differentiate them from other grades, such as toughness and ductility superior to other steels. They also have shallow temperatures; good mechanical and corrosion resistance at high temperatures; high hardening capacity due to plastic deformation; good weldability, among others [12].

Austenitic stainless steels, once subjected to high-temperature operations, may suffer from the phenomenon of sensitization, with the formation of chromium-rich carbides in the grain boundaries, becoming depleted of chromium in the surroundings, which weakens the steels, making them susceptible to intergranular corrosion [13]. Sensitization is the result of heat treatments, slow cooling through the sensitization range, working conditions in this range, welding operations, among others [14]. Sensitization represents the loss of

corrosion resistance in austenitic stainless steel by the formation of a depleted chromium zone within or close to the grain contour [15-16]. Sensitization occurs when the

intergranular precipitation of chromium carbides and the concomitant decrease in chromium in the regions adjacent to the grain boundaries, when austenitic stainless steels are primarily heated or cooled slowly through the temperature range between 450 °C and 850 °C, the maximum being about 650 °C [17-18]. The weakening of chromium in the grain boundary region leads to an increased susceptibility to intergranular corrosion [10]. The main types of carbides that can precipitate in austenitic stainless steels are $M_{23}C_6$, MC, M_7C_3 and M_2C [19]. This paper evaluated the behavior of AISI 314 steel at high temperatures and determined the reasons that led to the rupture. It also shows the response of AISI 314 steel at high temperatures and submitted to an atmosphere rich in hydrocarbons. AISI 314 steel has a high silicon content in its chemical composition, increasing resistance to oxidation at high temperatures. The material object of the present work consists of a metal link, a component of a conveyor belt in a heat treatment furnace.

II. EXPERIMENTAL METHOD

The investigated sample is a metal link belonging to a conveyor belt of a controlled atmosphere heat treatment furnace. The sample can be evaluated “before service” as it is the material before being subjected to the furnace's operating conditions, and “after service” if it is the material after going through the operating conditions of the same. Its chemical composition, as a rule, is shown in Table 1.

Table 1 - Chemical composition of AISI 314 steel [8].

Element	C	Mn	P	S	Si	Cr	Ni
	(max.)	(max.)	(max.)	(max.)	(max.)	(min.)	(min.)
						(max.)	(max.)
%	0,25	2,0	0,045	0,03	1,5	23,6	19,0
					3,0	26,0	22,0

The chosen samples come from a conveyor belt. The samples submitted to spectrometry tests before and after the service, Vickers Microhardness, MO, SEM with EDS, and Corrosion by immersion showed conclusive results. The verification of the constituent elements of AISI 314 steel, this before and after being subjected to an atmosphere rich in hydrocarbons, was carried out in an optical emission spectrometer. Table 2 shows the weight percentage composition of AISI 314 steel before use in service.

Table 2 - Chemical composition of AISI 314 steel before use in service.

Element	C	Si	Mn	P	S	Cr	Mo
%	0,145	3,34	1,37	0,022	0,073	22,9	0,224
	Ni	Al	Co	Cu	Nb	Ti	V
	18,8	0,0164	0,0911	0,589	0,0234	0,0089	0,0821
	W	Pb	Sn	B	Ca	Se	N
	0,0233	0,0025	0,025	0,0005	0,008	0,0035	0,722

The chemical composition verified meets the specifications of AISI 314 steel. There are no significant variations, and the typical composition of austenitic stainless steels is following the indication of some authors [20 – 21].

The chemical composition of the material after use in service is in Table 3 demonstrate.

Table 3 - Chemical composition of AISI 314 steel after the operation in an atmosphere wick hydrocarbons.

Elemento	C	Si	Mn	P	S	Cr	Mo
%	0,699	0,973	2,64	0,0343	0,097	25	0,436
	Ni	Al	Co	Cu	Nb	Ti	V
	23,2	0,23	0,227	1,76	0,127	0,0525	0,0938
	W	Pb	Sn	B	Ca	Se	N
	3	0,2	0,0062	0,025	0,008	0,0173	1

The sample prepared for embedding in the appropriate size was embedded in bakelite at a temperature of 120 ° C, remaining at this temperature for 40 minutes, and then cooled for removal from the machine.

The sample prepared to obtain a flat and shiny surface, with sandpapers in the following order of granulometry, 120, 220, 400, 500, 600, 800, 1000. The sample is rotated by 90 ° with each sanding change, to eliminate the scratches from the previous process, so until the last sanding operation. The parallelism between the upper and lower surfaces of the sample aimed to eliminate deviations resulting from the inhomogeneity of the pressure exerted on the sample.

After sanding, polishing the sample with abrasive grains followed a standard metallography sequence. The sample went to the microhardness test. The equipment is sensitive to the movement of the sample during the test, with the risk of breakage of the indenter, it must remain immobile, trying to avoid promoting any movement on the equipment bench.

The load used was 0.3 kg, maintained for 10 seconds. For the Vickers microhardness test, five indentations were performed per sample, in a total of six samples, with a load of 0.3 kg, which obtained a lower deformation in the indentation mark. The measurements were made starting from the surface of the samples and advancing towards the center, spaced 300 mm apart.

The microstructural analysis of the material occurred with the use of an optical microscope of reflected light with image acquisition. The scanning electron microscope (SEM) and semi-quantitative analysis by dispersive energy spectrometry (EDS), can be seen in the presence of precipitates or anisotropies. With immersion testing, a simple test among accelerated corrosion tests, it is possible to quickly assess the behavior of a material under a given service condition. These tests are very flexible and adapted to meet a specific situation.

In the immersion test, one of the practices to accelerate the material's behavior about corrosion is to increase the concentration of the corrosive agent. The most used corrosive agents are acids, chlorides, moisture, oxygen, among others. The immersion test is for when you need quick answers because, in general, you get the highest degree of corrosion in the shortest time. The immersion time of the material varies according to the type of material and the solution used for immersing the sample [21].

III. RESULTS AND DISCUSSION

In the Vickers microhardness test, the five sample indentations performed on the six samples. Figure 1 shows a comparison between the hardnesses for all samples.

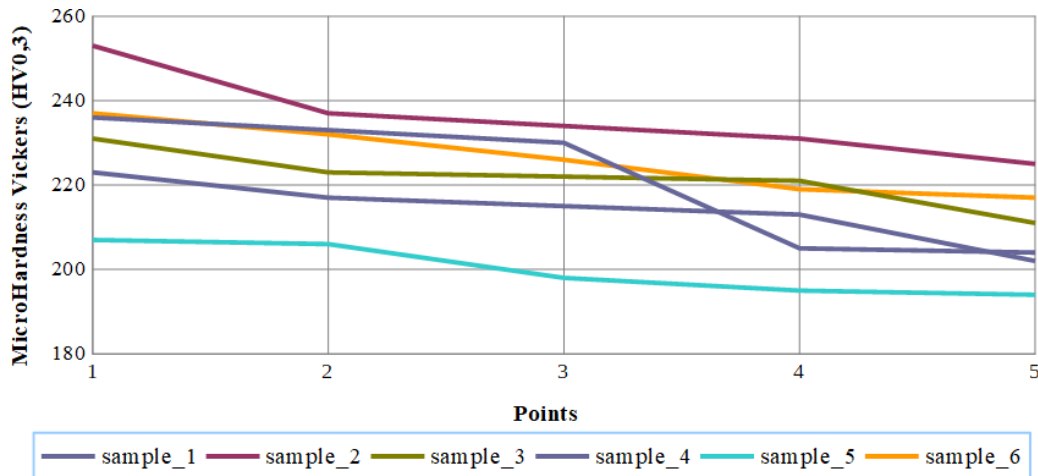


Figure 1 - Curve with the results of the Vickers microhardness test for all Samples.

Close to the surface, the presence of higher microhardness values than the core was verified, indicating carbon enrichment. Through the hardness tests, it was possible to verify that the hardness in all the samples had a decline as it progresses in indentations from 1 to 5 (surface - center), indicating carbon diffusion from the surface, weakening the Sample.

The images obtained by optical microscopy are shown in Figures 2 and 3, being in several magnifications. In all samples, the presence of precipitates detected in the grain boundaries. The presence of these precipitates contributes significantly to the reduction of corrosion resistance and the weakening of steel [21].

In Figure 2, it is possible to identify the chromium carbides, characteristic of sensitized stainless steel, next to the precipitated grain contours.

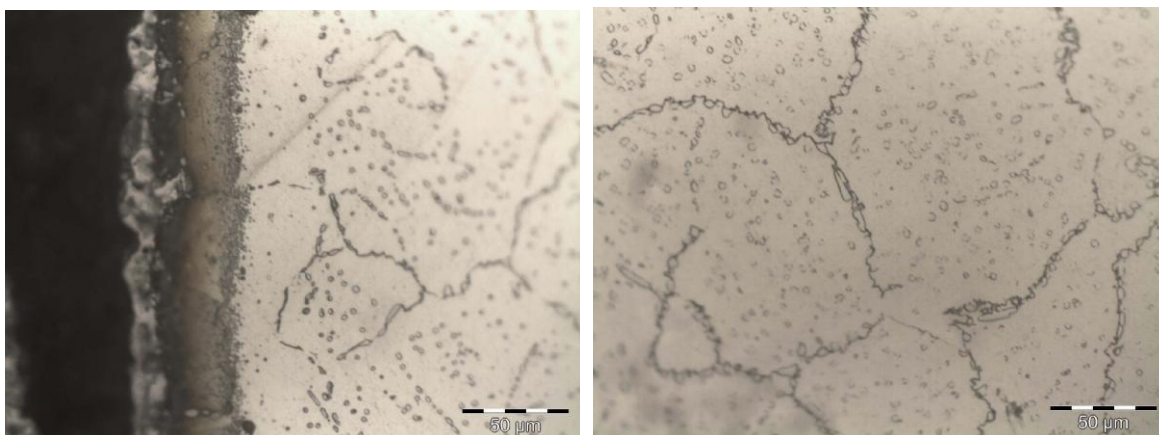


Figure 2 - Presence of precipitates near the grain boundaries.

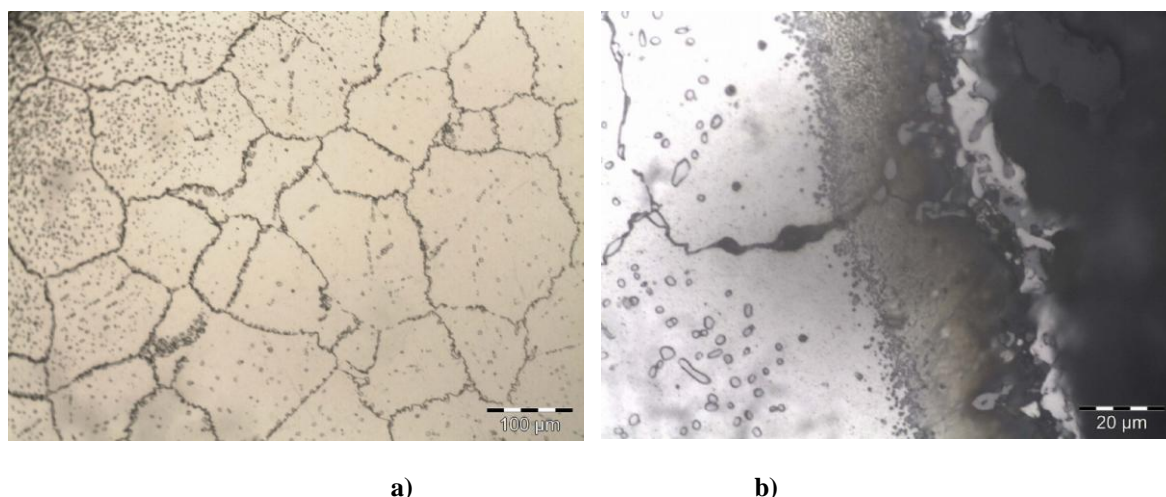


Figure 3 - a) Abnormal grain growth due to the high temperature applied. b) Anisotropy is typical of the degradation of stainless steel.

Figure 3 a) represents an abnormal growth of the grain due to the high temperature to which it subjected to the piece. In Figure 3 b), the precipitation of carbides of type $M_{23}C_6$ [21] is noticed, causing the depletion of chromium in the regions adjacent to the grain boundaries.

Evaluating the Figures 2 and 3 was verified the morphology of the same ones constituted by austenite with precipitates in the grain contours. This condition contributes significantly to the reduction of corrosion resistance, being following the literature. The presence of a degraded passive film typical of austenitic stainless steels subjected to the sensitization process was also verified [21].

Still, on the surface, the process of interstitial diffusion of carbon from the atmosphere used in hydrocarbon-rich furnaces is observed. The images obtained in the SEM and EDS tests reinforce the results obtained by MO.

Figures 4 show the images captured by SEM, and Figure 5 show the results obtained by EDS. It is verified in all the precipitated samples degrading the analyzed surfaces and the presence of corrosion pits. This condition is associated with the partial rupture of the chromium oxide layer and the reduction of the Cr content necessary for repassivation [3]. In Figure 4, the presence of precipitates observed, as well as the formation of corrosion pits.

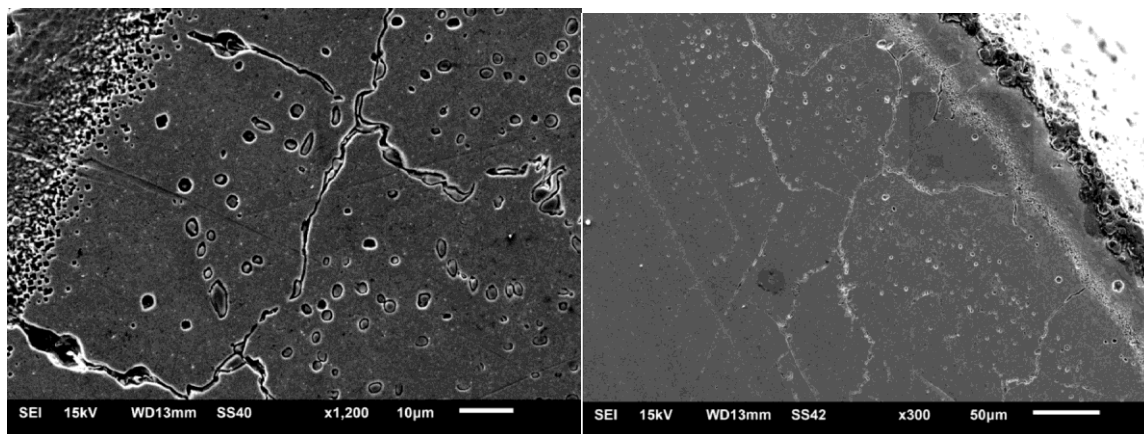


Figure 4 - Precipitated next to the grain contours.

In Figure 5, we see a decrease (segregation) of both chromium and silicon from the center of the piece to the surface. Interestingly, a value of less than 11% in Chromium was not found in the analyzes by DES, although it is evident the presence of the formation of precipitates, as well as the percentage of Si that remained between 1 to 3% in all analyzed portions. However, as widely reported in the literature, the EDS assay is qualitative, not quantitative.

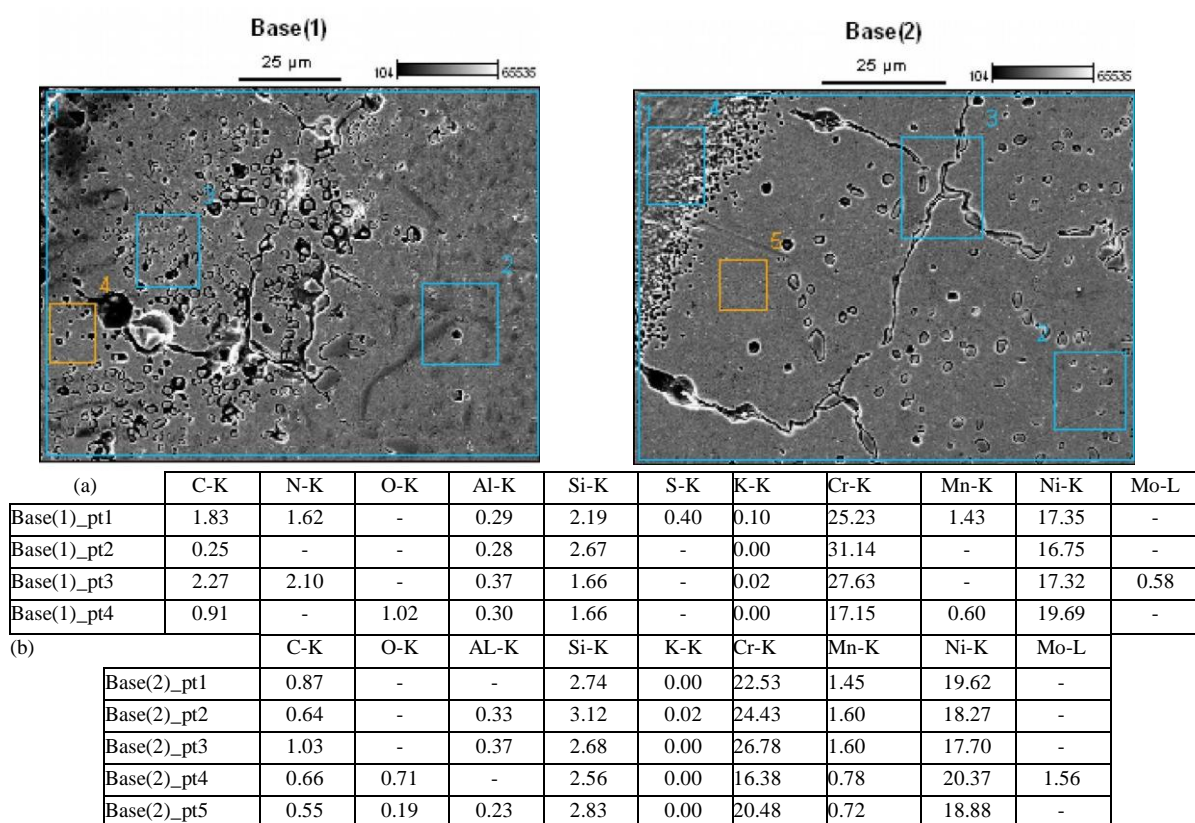
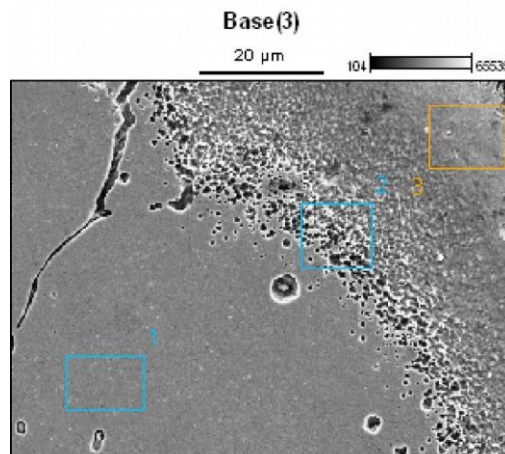


Figure 5 – Precipitated along the grain boundaries and surface degradation.

In Figure 5 b) a reduced amount of Chromium is also observed in Rectangle 4, closer to the surface of the piece compared to Rectangle 3 ($M_{23}C_6$), indicating a zone depleted in Chromium around carbides rich in this element, typical of sensitization, forming a micropile, where the chromium-rich region will be cathode and the poor anode, where it will corrode. Also, in Rectangle 3, we can see the high percentage of carbon compared to the other locations analyzed.



	C-K	O-K	AL-K	Si-K	S-K	K-K	Cr-K	Mn-K	Ni-K	Cu-K
Base(3)_pt1	0.41	-	0.28	2.66	-	0.13	22.73	1.71	18.90	-
Base(3)_pt2	1.37	2.17	0.28	2.52	0.59	0.13	17.99	1.32	19.23	-
Base(3)_pt3	0.70	1.45	-	2.36	1.13	0.07	14.55	-	20.15	3.80

Figure 6 - Precipitated next to the grain contours and superficial degradation.

In Figure 6, we can see the segregation of chromium and silicon towards the surface. For the immersion corrosion test, the sample was removed from bakelite, and then immersed in the NaCl solution, at room temperature, and showed signs of corrosion. The presence of corrosion in the sample was after 72 hours. This behavior indicates severe degradation of the passivated layer and reduction of Cr for repassivation. There is also a significant increase in nitrogen, which causes the austenitizing effect. The silicon reduced due to the atmosphere and the working temperature to which the sample was exposed.

Silicon contributes to reducing the sensitization of steels and increasing resistance to oxidation at elevated temperatures. However, the sample was exposed to a temperature above that indicated in the literature and in too long, so it caused a corrosive environment and caused the degradation of the material.

IV. CONCLUSIONS

The analyzed samples were worked at high temperatures (on average 1200 ° C). Due to their high silicon content, the samples should withstand temperatures above 1200 ° C in an oxidizing or reducing atmosphere. Temperature tolerance values tend to decrease in the case of more aggressive environments containing sulfur elements. The first component broke due to the chemical unbalance of the steel caused by the segregation of silicon and the precipitated chromium in the grain boundaries. The operating conditions and operating temperature of the component did not cause sensitization of the material.

Failures in the second component, as it had already gone through a sensitization process, caused the belt to weaken as a whole. The fact that the furnace operates at high temperature may have favored chromium carbides. However, the same would not happen with silicon carbides. So, even if chromium carbides were solubilized by the operating temperature, there would be silicon carbides. Therefore, it is evident that the material failed due to a combination of sensitization and manufacturing defect.

With the spectrometry of materials before and after their use, it was possible to prove the increase in carbon content. This change favored the degradation of materials such as carbon, molybdenum, boron and nitrogen, and contributed to the formation of precipitate M₂₃C₆.

With the spectrometry of the material - before and after its use in service, Vickers microhardness tests, immersion corrosion, SEM and EDS images generated the following conclusions:

- Carbon enrichment has occurred, after in-service use. The operating condition of the furnace in a hydrocarbon-based atmosphere and at a high temperature provided this effect;
- The increase in carbon contributed to a significant reduction in corrosion resistance, with sensitization being increased with carbon diffusion.

- The diffusion of carbon from the surface contributed to the embrittlement, detected by the presence of surface microcracks and by the reduction of hardness in the surface - center direction;
- Precipitated carbides were found in the grain contour, typical characteristics of sensitized stainless steel;
- In immersion corrosion tests, the material showed corrosion in 72 hours. This behavior indicates severe degradation of the passivated layer and reduction of chromium for repassivation;
- The increase in chemical elements such as carbon and nitrogen, in the material after its use in service, contributed to the degradation of the content;
- A decrease in both chromium and silicon towards the surface was observed. Although these elements remain in the minimum range indicated by the authors, the material suffered a break in the passivated layer and showed signs of corrosion, intergranular, and pitting.

REFERENCES

- [1]. LI, H., QIN, J., JIANG, Y., ZHOU, W., HUANG, H. Experimental study on the thermodynamic characteristics of the high temperature hydrocarbon fuel in the cooling channel of the hypersonic vehicle.
- [2]. Acta Astronautica. Volume 155, February 2019. Pages 63-79. DOI: 10.1016/j.actaastro.2018.11.021
- [3]. OLIVEIRA, R. C. L. M., BIEHL, L. V., MEDEIROS, J. L. B., FERREIRA FILHO, D., SOUZA, J.
- [4]. D. Comparative analysis between quenching and partitioning versus quenching and tempering for SAE 4340 [in Portuguese]. *Matéria* (Rio de Janeiro), Volume 24 Issue 3 (2019). DOI: 10.1590/S1517-707620190003.0788
- [5]. SANTOS JR, A. G., BIEHL, L. V., ANTONINI, L.M. Effect of chemical passivation treatment on pitting corrosion resistance of AISI 430 and AISI 316L stainless steels [in Portuguese]. *Matéria* (Rio de Janeiro), v. 23, n. 1, 2018. DOI:10.1590/s1517-707620170001.0293
- [6]. STOKKERS, G. J., SILFHOUT, A. VAN, BOOTSMA, G. A., FRANSEN, T., GELLINGS, P. J. Interaction of oxygen with an AISI 314 stainless steel surface studied by ellipsometry and auger electron spectroscopy in combination with ion bombardment. *Corrosion Science*. Volume 23, Issue 3 1983 Pages 195-204 DOI: 10.1016/0010-938X(83)90102-6
- [7]. BORTOLOZZI, J. P., GUTIERREZ, L. B., ULLA, M. A. Synthesis of Ni/Al₂O₃ and Ni-Co/Al₂O₃ coatings onto AISI 314 foams and their catalytic application for the oxidative dehydrogenation of ethane. *Applied catalysis a-general*. Amsterdam: ELSEVIER SCIENCE BV, 2013. vol. 452, p. 179-188. ISSN 0926-860X
- [8]. WU, B., TANG, G., WANG, Z., WANG, L., GU, L. Boundary Tribological Behaviors of Untreated and Surface-Modified M50 Steel Lubricated by Fuel JP-10, *Tribology Transactions*, 61:3, 424-436, 2018 DOI: 10.1080/10402004.2017.1341009
- [9]. GALLINA, B., BIEHL, L. V., MEDEIROS, J. L. B., SOUZA, J. D. The influence of heat treatment on steels in Hardox® 500 and Strenx® 700 steels [in Portuguese]. *Revista Liberato* Volume 20, Issue 34, p. 113-240 (2019). DOI: 00.00000/rliberato.2019v20n34.p00
- [10]. OLIVEIRA, M. U.; BIEHL, L. V.; MEDEIROS, J. L. B.; AVELLANEDA, C. A. O.; MARTINS, C.
- [11]. O. D.; SOUZA, J. D.; SPORKET, F. Manufacturing against corrosion: Increasing materials performance by the combination of cold work and heat treatment for 6063 aluminium alloy. *Materials Science-Medziagotyra*, 2020. DOI: 10.5755/j01.ms.26.1.17683
- [12]. COZZA, L. M., SILVA JUNIOR, M. F., MEDEIROS, J. L. B., BIEHL, L. V., MARTINS, C. O. D., SOUZA, J. D. Effect of heat treatment for stress reduction on the microstructure and grain size of a micro-alloyed steel [in Portuguese]. *Revista Liberato* Vol. 19 Issue 31 (2018) pp. 57-65. DOI: 10.31514/liberato.2018v19n31.p57
- [13]. NAMA, N. D., PHUNG, V. D., THUY, P. T. P., DAO, V. A., KIMD, S. H., YI, J. S. Corrosion behaviours of hot-extruded Al-xMg alloys. *J. Mat. Res. Technol.* 2019; 8 (6):5246-5253. DOI: 10.1016/j.jmrt.2019.08.047
- [14]. GURUMURTHY, B. M., GOWRISHANKAR, M. C., SHARMA, S. KINI, A., SHETTAR, M., HIREMATH, P. Microstructure authentication on mechanical property of medium carbon Low alloy duplex steels. April 2020 DOI: 10.1016/j.jmrt.2020.03.027
- [15]. WANG, L., ZHANG, L., LUO, L. S., WANG, B., YAN, H., CHEN, R. R., SU, Y. Q., GUO, J. J. FU, H. Z. Effect of melt hydrogenation on microstructure evolution and tensile properties of (TiB + TiC)/Ti-6Al-4V composites. April 2020. DOI: 10.1016/j.jmrt.2020.03.047
- [16]. *Metals Handbook, Vol. 1: Properties and Selection. Irons, Steels and High Performance Alloys*. 10th ed, Materials Park, OH, USA, ASM, 1990.
- [17]. KOLLI, S., JAVAHERI, V., KÔMIA, J., PORTER, D. The importance of steel chemistry and thermal history on the sensitization behavior in austenitic stainless steels: Experimental and modeling assessment. *Materials Today Communications* In press, March 2020 Article 101088 DOI: 10.1016/j.mtcomm.2020.101088
- [18]. REZENDE, S. C. Estudo do Mo na microestrutura e na resistência à corrosão em aço inoxidável duplex. *Disertação de Mestrado – Universidade Federal de Alfenas – Campus Poços de Caldas – 2 Poços de Caldas/MG*, 2018.
- [19]. SILVEIRA, F. A., ZUCHETTO, A., RUPPENTHAL, J. E., MACHADO, F. M. ABNT 8640 Steel Quench Heat Treatment: Analysis of Mechanical Properties [in Portuguese]. *HOLOS*, Volume 34, Issue 2, p. 49-59, 2018. DOI: 10.15628/holos.2018.5614
- [20]. GHABUSSI, A., MARNANI, J. A., ROHANIMANESH, M. S. Improving seismic performance of portal frame structures with steel curved dampers. *Structures*. Volume 24, April 2020 Pages 27-40. DOI: 10.1016/j.istruc.2019.12.025
- [21]. DING, H., WU, W., LU, Q., ZHENG, J. A method for calculating low-temperature stress-strain curves of austenitic stainless steels. *Cryogenics* Volume 107, April 2020 Article 103059 DOI: 10.1016/j.cryogenics.2020.103059
- [22]. BORTOLOZZI, J. P., BANÚS, E. D., MILT, V. G., GUTIERREZ, L. B., ULLA, M. A. The significance of passivation treatments on AISI 314 foam pieces to be used as substrates for catalytic applications. *Applied Surface Science*. Volume 257, Issue 21 November 2010 Pages 495-502. DOI: 10.1016/j.apsusc.2010.07.019
- [23]. MORRIS, Garron K.; GENTHE, Christopher; LUKASZEWSKI, Richard A. Challenges And Best Practices In Mixed Flow Gas Corrosion Testing Of Electronics. In: 2019 Annual Reliability and Maintainability Symposium (RAMS). IEEE, 2019. p. 1-7. DOI:10.1109/RAMS.2019.8768973
- [24]. SUNDQVIST, J., MANNINEN, T., HEIKKINEN, HANNU-P., ANTTILA, S. Laser surface hardening of 11% Cr ferritic stainless steel and its sensitisation behaviour. *Surface and Coatings Technology*, v. 344, p. 673-679, 2018. DOI: 10.1016/j.surfcoat.2018.04.002
- [25]. CARDARELLI, François. *Materials Handbook*. London: Springer, 2018.